



Slow diffusion on the monolayer culture enhances auto/paracrine effects of Noggin in differentiation of human iPSCs induced by BMP

Eri Nakatani^a, Riho Okajima^b, Kiyoshi Ohnuma^{a,b,*}

^a Department of Science of Technology Innovation, Nagaoka University of Technology, 1603-1, Kamitomioka-machi, Nagaoka, 940-2188, Japan

^b Department of Bioengineering, Nagaoka University of Technology, 1603-1, Kamitomioka-machi, Nagaoka, 940-2188, Japan

ARTICLE INFO

Keywords:

Pattern formation
Reaction-diffusion
BMP4
Noggin secretion
Heparan sulfate proteoglycan

ABSTRACT

Auto/paracrine factors secreted from cells affect differentiation of human pluripotent stem cells (hPSCs). However, the molecular mechanisms underlying the role of secreted factors are not well known. We previously showed that pattern formation in hPSCs induced by BMP4 could be reproduced by a simple reaction-diffusion of BMP and Noggin, a cell-secreted BMP4 inhibitor. However, the amount of Noggin secreted is unknown.

In this study, we measured the concentration of Noggin secreted during the differentiation of hPSCs induced by BMP4. The Noggin concentration in the supernatant before and after differentiation was constant at approximately 0.69 ng/mL, which is approximately 50–200 times less than expected in the model. To explain the difference between the experiment and model, we assumed that macromolecules such as heparan sulfate proteoglycan on the cell surface act as a diffusion barrier structure, where the diffusion slows down to 1/400. The model with the diffusion barrier structure reduced the Noggin concentration required to suppress differentiation in the static culture model. The model also qualitatively reproduced the pattern formation, in which only the upstream but not the downstream hPSCs were differentiated in a one-directional perfusion culture chamber, with a small change in the amount of secreted Noggin resulting in a large change in the differentiation position. These results suggest that the diffusion barrier on the cell surface might enhance the auto/paracrine effects on monolayer hPSC culture.

1. Introduction

Auto/paracrine factors secreted from cells largely affect the differentiation and fate of the secreting cells as well as the surrounding cells both in vivo and in vitro. The auto/paracrine factors affect both three-dimension (3D) culture (spheroid or embryoid body) and two-dimension (2D) culture (monolayer culture) of human pluripotent stem cells (hPSCs), including embryonic stem cells and induced pluripotent stem cells [1,2]. Because of this, high initial cell density culture is frequently used to induce specific cells by enhancing cell-cell interactions mediated by auto/paracrine factors [1,3,4]. However, the molecules that function as auto/paracrine factors and the mechanisms underlying the release, movement, and reaction of these molecules are not fully understood.

Auto/paracrine factors are thought to induce spatial pattern formation during the differentiation of monolayered cultured hPSCs [5]

although the diffusion in the medium is much faster than in the inside of the 3D culture. For example, discoidal hPSC colonies of approximately 100 μm –1 mm form concentric circular patterns of differentiated cells induced by bone morphogenic proteins (BMPs). BMPs are TGF- β superfamily molecules that play essential roles in the differentiation of multiple types of cells and embryonic pattern formation, such as dorsal-ventral axis formation. During the formation of the concentric circular pattern, Noggin, a BMP inhibitor, that is secreted from cells may play a major role in reaction-diffusion with BMPs [6,7]. Noggin is a signaling molecule that is synthesized and secreted by the Spemann organizer of the amphibian gastrula [8,9]. Noggin is induced by BMPs and also inhibits BMPs, which induce neural tissue and determine the dorsal position of the mesoderm [8,10]. In addition, Noggin acts in hPSC differentiation. It has been reported that Noggin is secreted on the apical side of cells, which corresponds to the amniotic side of the human embryonic disc [11]. These results suggest that the auto/paracrine effects

Abbreviations: BMP, bone morphogenic protein; hPSCs, human pluripotent stem cells; HSPG, heparan sulfate proteoglycan.

* Corresponding author. Department of Science of Technology Innovation, Nagaoka University of Technology, 1603-1, kamitomioka-machi, Nagaoka, 940-2188, Japan.

E-mail address: kohnuma@vos.nagaokaut.ac.jp (K. Ohnuma).

<https://doi.org/10.1016/j.bbrep.2021.101195>

Received 8 October 2021; Received in revised form 20 December 2021; Accepted 20 December 2021

2405-5808/© 2021 The Authors. Published by Elsevier B.V. This is an open access article under the CC BY-NC-ND license

(<http://creativecommons.org/licenses/by-nc-nd/4.0/>).

of Noggin may affect the pattern formation of hPSCs through inhibition of BMPs.

We have previously shown that BMP4 induced differentiation in cultured hPSCs at a low initial cell density, but not at a high initial cell density, and also demonstrated that BMP induced differentiation only upstream, but not downstream in hPSCs in a one-directional perfusion culture chamber [12]. These results suggest that the cells secrete BMP4 inhibitors, such as Noggin, which act as an auto/paracrine factors by suppressing BMP4. Thus, we assume that the cells secrete Noggin, which diffuses and reacts with externally added BMP4 to inhibit its action, forming a cell differentiation pattern. Based on this assumption, we solved three reaction-diffusion equations for externally added BMP, the secreted Noggin, and the inactive Noggin-BMP4 complex [13]. However, we did not experimentally measure Noggin secretion.

In this study, we measured Noggin concentration in the supernatant of BMP4-induced differentiated hPSCs using an enzyme-linked immunosorbent assay (ELISA). Based on the measured concentrations, we developed a new model to better explain the effects of Noggin as an auto/paracrine factor. In the new model, we assumed that ubiquitous cell surface macromolecules of adherent cells, such as heparan sulfate proteoglycans (HSPGs), slowed down the diffusion of signal molecules by binding to them [14–16]. Our working hypothesis is that the cell surface macromolecules trap the secreted Noggin near the cell surface to enhance its auto/paracrine effects. This suggests that a small amount of Noggin could suppress a large concentration of BMP added to the medium. We tested the hypothesis using a numerical simulation.

2. Materials and methods

2.1. Culture of human iPSCs

The hPSC cell line 201B7 [17] was obtained from the RIKEN BRC Cell Bank (HPS0063, Tsukuba, Japan) via the National Bio-Resource Project for MEXT, Japan. Cells were cultured in maintenance medium (StemFit AK02 N, Ajinomoto, Tokyo, Japan) with Y-27632 (Rock inhibitor, final concentration 5 μ M, 036–24023, Wako) and 2.5 μ g/cm² laminin (iMatrix-511-silk, Nippi, Tokyo, Japan) being used for passage according to the manufacturer's protocol. For passage of cells, TrypLE (TrypLE select (1 \times), 12563-011, Thermo Fisher Scientific K.K., Massachusetts, USA) was used.

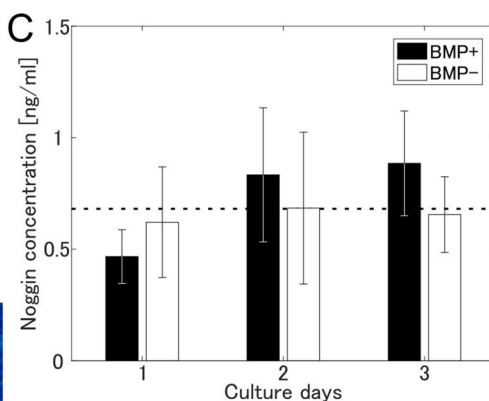
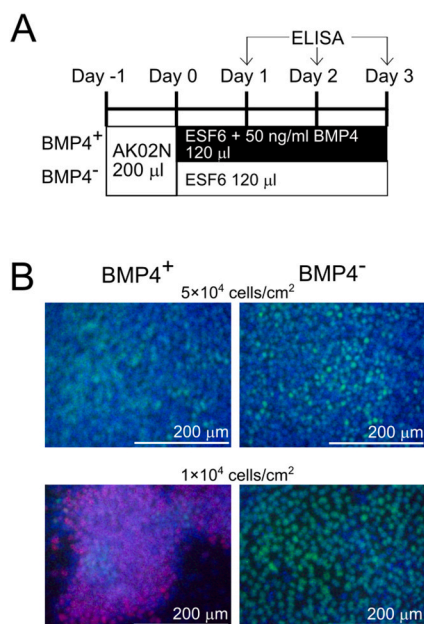


Fig. 1. ELISA of Noggin in the supernatant.

(A) Schematics of the experiment. Cells were either exposed to (black) or not given (white) BMP4 and the supernatant was harvested for ELISA at day 1, 2, and 3 (arrows). (B) Immunostained cells cultured with (left) and without (right) BMP4 conditions at day 3. SOX2 (green): undifferentiated marker. Brachyury (red): mesoderm marker. DAPI (blue): nuclei. Initial cell densities were 1 \times 10⁴ and 5 \times 10⁴ cells/cm². (C) Noggin ELISA results. Four Noggin concentrations in independent supernatants were collected from different cell cultures at different passages. The vertical axis is Noggin concentration in the supernatant. (Mean \pm S.E., n = 4). The horizontal dotted line indicates the mean of all the data (0.69 ng/mL). (For interpretation of the references to colour in this figure legend, the reader is referred to the Web version of this article.)

2.2. ELISA analysis and immunostaining

The cells were seeded in 96 well plates at a density of 5 \times 10⁴ cells/cm² under maintenance conditions (day –1) in AK02 N medium. On the day after seeding (day 0), the media was replaced with 120 μ L of ESF6 (supplementary table TS1) with or without 50 ng/mL BMP4. The culture supernatant (120 μ L) was collected, cryopreserved, and replaced with 120 μ L of fresh medium at days 1, 2, and 3 (Fig. 1A). The supernatants were thawed and centrifuged at 1000 \times g for 2 min to measure Noggin using an ELISA Kit (SEC130Hu, Cloud Clone Corp., Houston, USA) according to the manufacturer's instructions. The absorbance was measured at 450 nm using a microplate reader (Model 680, Bio-Rad, Hercules, CA, USA).

For immunostaining, the same cells were fixed with 4% paraformaldehyde(163–20145, Wako, Osaka, Japan) on day 3. The cells were permeabilized and blocked with blocking buffer consisting of phosphate-buffered saline (PBS), 0.2% Triton X-100, and 1% bovine serum albumin (BSA) (019–27051, Wako, Osaka, Japan). The cells were then incubated with primary and secondary antibodies in blocking buffer. The antibodies used are listed in Supplementary Table TS2. Cells were imaged using a fluorescent microscope (BZ-8100; Keyence, Osaka, Japan).

2.3. Simulation

We performed a numerical simulation of the distribution of substances and their concentrations in culture chambers as described previously [13]. Briefly, BMP4 and Noggin react one by one to produce the BMP4- Noggin complex (BMP4-Noggin), which is an inactive form of BMP4, and these signal proteins diffuse as follows:

$$\frac{\partial[N]}{\partial t} = D_N \nabla^2 [N] - \mathbf{q} \cdot \nabla [N] - k_1 [N][B] + k_2 [NB]$$

$$\frac{\partial[B]}{\partial t} = D_B \nabla^2 [B] - \mathbf{q} \cdot \nabla [B] - k_1 [N][B] + k_2 [BN]$$

$$\frac{\partial[BN]}{\partial t} = D_{NB} \nabla^2 [BN] - \mathbf{q} \cdot \nabla [BN] + k_1 [N][B] - k_2 [BN]$$

where t is time, D_N , D_B , and D_{BN} are the diffusion coefficients of the Noggin, BMP4, and BMP4-Noggin complexes, respectively, and \mathbf{q} is the

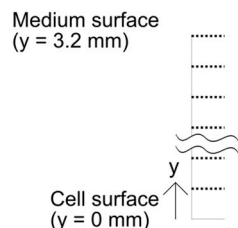
flow velocity used in our previous study using a one-directional perfusion microchamber [12]. These equations were solved every 0.5 s using a finite-difference method on a $20 \mu\text{m} \times 20 \mu\text{m}$ uniform mesh. All parameters are listed in the Supplementary Information (Supplementary Table TS3). We assumed that cells had differentiated to express the marker protein when [total exposed BMP], which is an integrated value for BMP4 concentration on the cell surface, which is initially zero ($t = 0$ s), exceeded 100 h ng/mL BMP4 . To estimate the Noggin concentration in the supernatant of the culture medium, the $[N (y_{\min} < y < y_{\max})]$ was calculated as the average Noggin concentration between y_{\min} and the medium surface ($y = y_{\max}$). x and y are the horizontal and vertical directions of the culture vessel, respectively. For the static culture condition, we assumed that the width direction of the culture space was uniform; thus, the simulation space was a 1-dimensional line (y). The medium flow velocity, q , was zero. Medium change was expressed by resetting the values of signal molecules above the diffusion varies with 10 or 50 ng/mL BMP4, 0 ng/mL Noggin and 0 ng/mL Noggin-BMP at $t = 24$ and 48 h. For perfusion culture conditions, the simulation space was a 2-dimensional cross-section perpendicular to the floor with a height of 2 mm and length of 7 mm corresponding to half of the actual chamber length. The simulation was performed until $t = 72$ h. The medium flowed from upstream to downstream.

3. Results

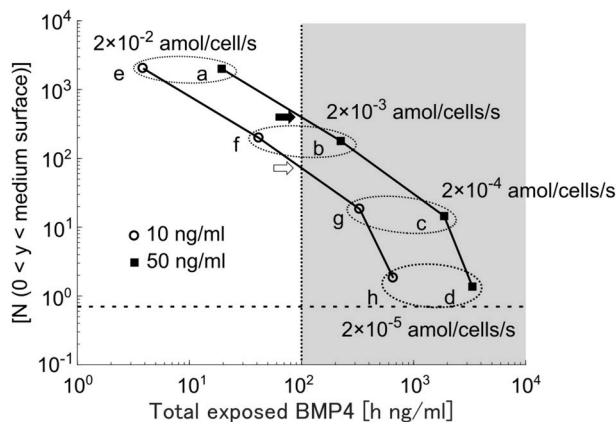
3.1. ELISA analysis of the supernatant of cells differentiated by BMP induction

We cultured hPSCs with or without BMP4 under serum- and feeder-free conditions, which did not contain Noggin. Although BMP4 induced cell differentiation (SSEA-1 positive) at an initial low cell density condition, the cells remained undifferentiated (SOX2 positive) at an initial high cell density condition, suggesting the cells secreted inhibitor (Fig. 1B). Thus, we measured secreted Noggin in the supernatant by ELISA under the initial high cell density condition (Fig. 1A). We found that the mean concentration of Noggin was in the range of 0.46–0.89 ng/mL on all three days both with and without BMP4, and that the mean value of all six conditions was 0.69 ng/mL (Fig. 1C). There were no significant differences between the mean value of all six conditions and that of each condition ($P = 0.54$ – 0.99 , two tailed Student's t-test), suggesting that there was no change in secreted Noggin. Based on these results, we presume that the cells secreted approximately 0.69 ng/mL Noggin constantly, regardless of the presence or absence of BMP4 for three days.

A static culture



B



3.2. Simulation of simple static culture

We previously reported that simulation with constant Noggin secretion could reproduce our experimental results that cells differentiated at a low initial cell density (5×10^3 cells/cm²), but not at a high initial cell density (5×10^4 cells/cm²) [13]. In the simulation, we assumed that the amount of secreted Noggin was approximately 100 ng/mL based on neural differentiation, which requires inhibitors of the TGF- β family, including BMP inhibitors such as Noggin [18]. However, our measurement of Noggin was approximately 0.69 ng/mL (Fig. 1C), which is approximately 1/145 of the value we have used in our previous simulation.

To numerically compare the results of the simulation and experiment, we used a scatter plot in which the abscissa is the total exposed BMP4, which is a criterion of differentiation, and for which the ordinate is the average concentration of Noggin in the medium (Fig. 2B). The right side of the threshold level of total exposed BMP4, which was set at 10^2 h ng/mL (vertical line in Fig. 2B), is the differentiated area. The average concentration of Noggin was $[N (0 < y < y_{\max})]$, which is different from Noggin secreted from the cells because the reaction with BMP4 reduces Noggin concentration and diffusion of Noggin causes a spatially non-uniform distribution. A horizontal line at $[N (0 < y < y_{\max})] = 0.69 \text{ ng/mL}$ corresponds to the ELISA results (Fig. 1C). If the simulated $[N (0 < y < y_{\max})]$ is close to the horizontal line, this suggests that the simulation can reproduce the experimental result (Fig. 2B).

First, we calculated the $[N (0 < y < y_{\max})]$ and total exposed BMP4 at the condition that the secreted Noggin from the cell was between 2×10^{-2} and 2×10^{-5} amol/cell/s (a is atto or 10^{-18}) and the medium contained 50 ng/mL BMP4. As the high initial cell density condition has ten times more cells, the cells secrete ten times more Noggin than the low initial cell density condition. The right and left points of the neighboring two points in the figure correspond to the low and high initial cell density conditions, respectively (Fig. 2B). For example, 2×10^{-2} and 2×10^{-3} amol/cell/s (closed rectangles a and b in Fig. 2B) correspond to high (2×10^{-2} amol/cell/s) and low (2×10^{-3} amol/10 cell/s) initial cell density conditions with 2×10^{-3} amol/cell/s secreted Noggin, and these two conditions are undifferentiated and differentiated, respectively. The value $[N (0 < y < y_{\max})]$ at the crossing point with the threshold line (closed arrow in Fig. 2B) was approximately 200 ng/mL, indicating that simulation results requires 290 times more Noggin secretion than the experimental result. Then, we evaluated another experimental condition, 10 ng/mL BMP4, where the cells differentiated in a way similar as that in the 50 ng/mL BMP4 condition [12]. Between 2×10^{-3} and 2×10^{-4} amol/cell/s secretion (open circles f and g in Fig. 2B), the line crossed the threshold, where $[N (0 < y < y_{\max})]$ was approximately 50 ng/mL (open arrow in Fig. 2B), indicating that 72 times more Noggin is required compared to the experimental

Fig. 2. Simulation of the simple static culture.

(A) Scheme of the simulation of static culture. The cells are placed at the bottom ($y = 0$), which is covered with the culture medium ($y > 0$). Each square is $20 \mu\text{m}$ by $20 \mu\text{m}$. (B) Scatter plot of the spatially averaged $[N(y)]$ concentration in the medium ($y > 0$) and total exposed BMP4 at $t = 72$ h when the barrier-like structure was not applied under each condition. The open circles and closed rectangles represent 10 and 50 ng/mL BMP4 concentrations, respectively. Vertical dotted line indicates the threshold of cell differentiation (100 h ng/mL) and the right of the line correspond to differentiated cells (gray). Horizontal dotted line indicates the measured level of Noggin (0.69 ng/mL). The open and closed arrow are the crossing points between the undifferentiated and differentiated area.

result. These simulation results suggest that our simple reaction-diffusion model cannot explain our experimental results.

3.3. Effects of diffusion barrier in the static culture

To reduce the gap between our ELISA results and the model, we assumed a diffusion barrier on the cell surface in our model. Many signaling molecules, including BMPs and Noggin, bind to cell surface macromolecules such as HSPG and nucleic acids [19–22]. On binding of Noggin to HSPGs, its functional binding with BMPs is retained and its diffusion is slowed down [15]. The bindings of Noggin and HSPBs are not being unbound at physiological salt concentrations [15]. It has also been reported that the diffusion coefficient of Noggin falls to 1/400 ($0.2 \mu\text{m}^2/\text{s}^2$) compared to that in water at the surface of Heparin beads [23]. Thus, our working hypothesis is as follows: Cell surface macromolecules such as HSPGs slow down the diffusion of Noggin, BMP4, and Noggin-BMP4 complex on the cell surface, and, thus, the concentration of secreted Noggin and Noggin-BMP4 complex at the cell surface may be increased to suppress BMP4-induced cell differentiation, and the Noggin concentration of the supernatant, which is the remaining Noggin unbound to the HSPGs, may become low (Fig. 3A).

To test our hypothesis, we assumed that the diffusion coefficient of each signal molecule, Noggin, BMP4, and Noggin-BMP4 complex became 1/400 on the cell surface. In addition, inside the barrier, all the Noggin was exist but BMP4 did not initially ($t = 0$), because cells were cultured in BMP4-free medium one day before applying BMP4. We set the diffusion barrier thickness to 0, 20, 40, 80, and 160 μm . The simulation results showed that the y-axis (Noggin concentration in the supernatant) at the closing point with the vertical line (total exposed BMP4 = 10^2 h ng/mL) was approximately 25, 8, 2.2, and 0.6 with 20, 40, 80, and 160 μm barriers, respectively (Fig. 3C). The results suggest that 20 μm barrier on the cell surface requires 36-fold BMP4 inhibitor secretion, or the 80–160 μm barrier is sufficient for reproducing experimental results. Furthermore, we also simulated a diffusion constant of 1/1000 of the water (Fig. 3D). The simulation results showed that the y-axis at the closing point with the vertical line was approximately 7.3, 2, 0.6, and 0.1 with 20, 40, 80, and 160 μm barriers, respectively. The results suggest that 20 μm barrier on the cell surface need 11-fold BMP4 inhibitor secretion, or a 40–80 μm barrier is

sufficient for reproducing experimental results. Thus, the above results suggest that the diffusion barrier assumption effectively suppressed the Noggin concentration in the supernatant in the simulation for it to be close to the experimental results.

3.4. Effects of diffusion barrier in the perfusion culture

We also applied a barrier-like structure to simulate our previous experiment using a one-directional perfusion microchamber [12]. In our previous study, hPSCs were cultured with BMP4 in a one-directional perfusion culture chamber, in which proteins were transported unidirectionally (Péclet number was approximately 30). At high density, the cells within several millimeters upstream, but not downstream, express differentiation markers at 72 h of differentiation, suggesting that some autocrine/paracrine factors inhibit the action of BMP4 downstream [12]. This result was also confirmed by a simulation with constant Noggin secretion [13]. We further applied the diffusion barrier assumption to confirm our hypothesis (Fig. 4A and B).

Because we do not know the flow rate reduction in the HSPG, we simply set the number to keep the Péclet number the same (i.e., the flow rate also reduced to 1/400 of the water). The Noggin secretion rate from the cells changed from 2×10^{-4} to 2×10^{-3} , based on the static culture results (Fig. 3C). Without a diffusion barrier, although all of the areas were differentiated at 2×10^{-4} amol/cell/s Noggin, approximately 5, 2, and 1 mm of the upstream cells were differentiated at 5×10^{-4} , 1×10^{-3} , and 2×10^{-3} amol/cell/s Noggin, respectively, suggesting that the experimental results could be reproduced with a broad range of Noggin secretion rates. With 20 and 40 μm diffusion barriers, approximately 2 and 5 mm of the upstream cells were differentiated at 1×10^{-3} and 2×10^{-3} amol/cell/s Noggin, respectively, suggesting that the experimental results could be reproduced even though the concentration range of Noggin secretion rate was narrow. With the 160 μm diffusion barrier, although all the area was differentiated at 2×10^{-4} amol/cell/s, most of the area, except for 0.2 mm of the upstream cells was undifferentiated at 5×10^{-4} and 2×10^{-3} amol/cell/s Noggin, suggesting that the experimental results could be reproduced within the narrow range between the two Noggin secretion rates. The higher the barrier, the larger was the change in differentiation position (exceeding the threshold level) with the narrow range of Noggin secretion rates, suggesting that the diffusion

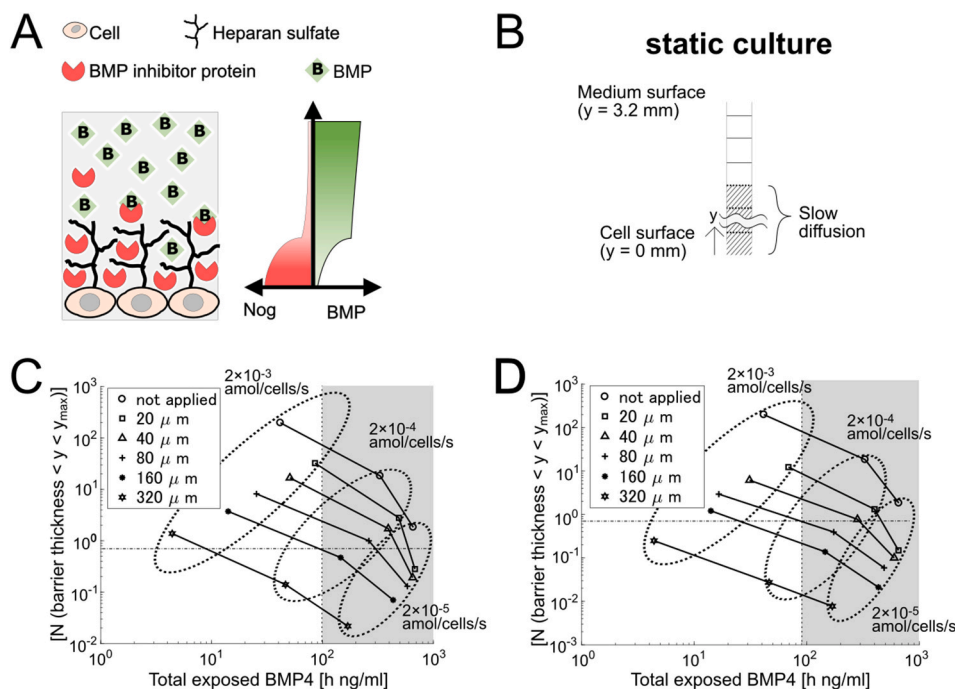


Fig. 3. Simulation of the static culture with diffusion barrier

(A) Scheme of the barrier structure with HSPG. (B) Scheme of the simulation. The cells are placed at the bottom ($y = 0$), which is covered with the culture medium ($y > 0$). Each square is 20 μm by 20 μm . Striped area is barrier-like structure where the diffusion is slow. Diffusion constants of Noggin, BMP4, and Noggin-BMP4 are 1/400 in the diffusion barrier.

(C) Scatter plot of $[N \text{ (barrier thickness } < y < y_{\text{max}})]$ and total exposed BMP4 at $t = 72 \text{ h}$ when the barrier-like structure was applied from $y = 0$ to 0 (no barrier), 40, 80, 160, and 320 μm and not applied. The diffusion in the barrier was set to 1/400 in B and 1/1000 in C. Vertical dotted line indicates the threshold of cell differentiation. Horizontal dotted line indicates $[N \text{ (barrier thickness } < y < y_{\text{max}})]$. The concentration was 10 ng/mL and the medium volume was 200 μL .

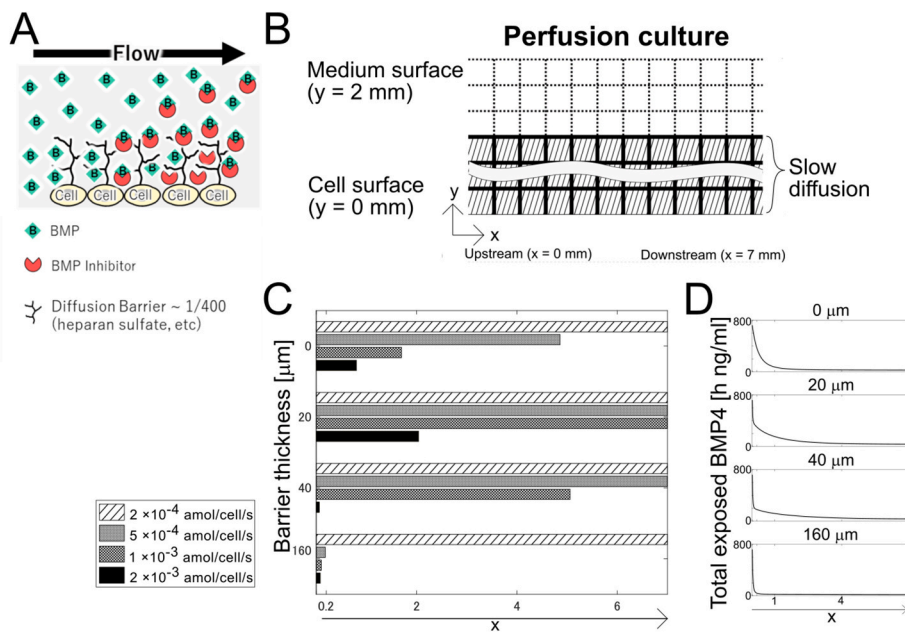


Fig. 4. Simulation of the unidirectional perfusion culture with diffusion barrier (A) Scheme of the barrier structure with HSPG. (B) Schematics of the simulation of perfusion culture. The cells placed at the bottom ($y = 0$) are covered with the culture medium ($y > 0$). The medium flows in at $x = 0$ and flows to x direction. Each square is $20 \mu\text{m}$ by $20 \mu\text{m}$. The shaded area denotes the diffusion barrier area where the diffusion and flow were $1/400$. (C) The area of the differentiated cells from the upstream is shown. The vertical axis is diffusion barrier thickness of 0 (not applied), 20 , 40 , and $160 \mu\text{m}$. The horizontal axis is the area of differentiated cells. (D) Total exposed BMP4 at $t = 72$ h. The vertical axis is total exposed BMP4. The horizontal axis is distance from the upstream.

barrier sharply changes or reduces the robustness of the pattern formation of cell differentiation and undifferentiation. These results suggest that although the simulation with a diffusion barrier could reproduce the experimental results, the robustness of pattern formation decreased with a higher barrier structure.

4. Discussion

We assumed that diffusion significantly slowed down on the cell surface. Many signaling molecules, including BMPs and Noggin, bind not only to HSPG, but also to many macromolecules, including proteoglycans, proteins, and nucleic acids, all of which exist on the cell surface and in the surrounding extracellular matrix [20,21]. Although the K_d of Noggin and these macromolecules is in the range of 10^{-5} – 10^{-7} M, 1 ng/mL Noggin is approximately 10^{-11} M, suggesting that Noggin is not tightly bound to cell surface macromolecules. Thus, the diffusion coefficient of Noggin falls to $1/400$ because of frequent binding and release. It has also been reported that ring pattern differentiation in the circular colony of hPSCs can be simulated by lowering the degradation rate of Noggin on the cell surface, which includes not only literary degradation but also decreases caused by vertical diffusion [6]. In addition, Wnt signaling proteins, which is another major signaling pathway, also bind HSPG on the cell surface [19,22]. Thus, there is a possibility that a hypothetical structure retains auto/paracrine factors significantly longer on the cell surface than mere diffusion in the medium and works as a diffusion barrier or source of alternative signaling molecules. The hypothetical structure may enhance the effects of auto/paracrine factors to strengthen the signal feedback (e.g., BMP4 induces Noggin, and Noggin suppresses BMP4 activity). This hypothesis is supported by the fact that simulation with a barrier-like structure could bring the observed Noggin concentration required for differentiation patterning in the experiments closer to the measured value; however, the measured Noggin concentration was insufficient without the barrier.

Although our current reaction-diffusion model with a diffusion barrier structure on the cell surface succeeded in partially explaining the experimental results, there are many limitations. First, our previous experiment showed that both 10 and 50 ng/mL BMP4 induced the same level of differentiation. However, the application of 50 ng/mL BMP4 induced differentiation five times earlier than 10 ng/mL BMP in our simulation. It has been reported that there is a difference in spatial

competence originating from BMP receptor localization [6,11]. Thus, loss of competency (the cells lose their ability to receive BMP4) must be employed. Second, although a barrier-like structure with a height greater than $80 \mu\text{m}$ may be unrealistic and $20 \mu\text{m}$ may be realistic, the lower barrier did not sufficiently suppress the Noggin concentration. Third, the diffusion barrier reproduced the perfusion culture results, but the results were not robust against the secretion amount. The second and third limitations may be partially overcome if there are more BMP4 inhibitors. Proteomic analysis of the supernatant during cardiac differentiation induced by Wnt activation from hPSCs shows that more than 10 factors are secreted and affect Wnt, FGF, Nodal, TGF β , and BMP signals [22]. Thus, it is possible that BMP4 also induces the secretion of these factors to suppress BMP4 10 times more than suppression level of Noggin. Thus, secretome analysis might be needed for BMP4 induced differentiation, which may be a future study. Fourth, although HSPG slows down the diffusion of signaling molecules, HSPG promotes the activity of signaling molecules, including BMP4 [24,25], which may increase the required Noggin concentration to inhibit BMP4. Fifth, we did not measure the effects of the addition of soluble heparin, which enables the immediate release of Noggin from the cell surface [15]. Because we used serum- and feeder-free culture conditions without heparin, simple addition of heparin may enable the measurement of total released Noggin from the cell, which is a topic that studies should investigate in the future.

5. Conclusion

Cells secreted Noggin at concentration of approximately 0.69 ng/mL , which was not sufficient to suppress BMP4 action in the culture medium. However, the existence of a diffusion-barrier-like structure, which slows down the diffusion of signaling molecules, on the cell surface could enhance the inhibitory effects of Noggin on BMP-induced cell differentiation. This structure might contribute to the formation of spatial differentiation patterns in monolayer cultured hPSCs.

Declaration of competing interest

The authors declare that they have no known competing financial interests or personal relationships that could have appeared to influence the work reported in this paper.

Acknowledgements

We would like to thank Editage (www.editage.com) for English language editing. This work was supported in part by grants from the Kosé Cosmetology Research Foundation (grant number J-19-18, to K. O.), and from the Terumo Life Science Foundation (grant number 20-III246 to K.O.). The funding bodies had no role in the study design, data collection and analysis, decision to publish, or preparation of the manuscript.

Appendix A. Supplementary data

Supplementary data to this article can be found online at <https://doi.org/10.1016/j.bbrep.2021.101195>.

References

- [1] D.M. Titmarsh, J.E. Hudson, A. Hidalgo, A.G. Elefanty, E.G. Stanley, E. J. Wolvetang, J.J. Cooper-White, Microbioreactor arrays for full factorial screening of exogenous and paracrine factors in human embryonic stem cell differentiation, *PLoS One* 7 (2012), e52405.
- [2] M.C. Benson, D.C. McDougal, D.S. Coffey, The Application of Perpendicular and Forward Light Scatter to Assess Nuclear and Cellular Morphology, 1984, pp. 515–522. *Cytometry*.
- [3] D.E. Glaser, W.S. Turner, N. Madfis, L. Wong, J. Zamora, N. White, S. Reyes, A. B. Burns, A. Gopinathan, K.E. McCloskey, Multifactorial optimizations for directing endothelial fate from stem cells, *PLoS One* 11 (2016), e0166663.
- [4] M. Hemmingsen, S. Vedel, P. Skafte-Pedersen, D. Sabourin, P. Collas, H. Bruus, M. Dufva, The role of paracrine and autocrine signaling in the early phase of adipogenic differentiation of adipose-derived stem cells, *PLoS One* 8 (2013), e63638.
- [5] R.E. Davey, P.W. Zandstra, Spatial organization of embryonic stem cell responsiveness to autocrine gp130 ligands reveals an autoregulatory stem cell niche, *Stem cells* 24 (2006) 2538–2548.
- [6] F. Etoc, J. Metzger, A. Ruvo, C. Kirst, A. Yoney, M.Z. Ozair, A.H. Brivanlou, E. D. Siggia, A balance between secreted inhibitors and edge sensing controls gastruloid self-organization, *Dev. Cell* 39 (2016) 302–315.
- [7] I. Martyn, T.Y. Kanno, A. Ruvo, E.D. Siggia, A.H. Brivanlou, Self-organization of a human organizer by combined Wnt and Nodal signalling, *Nature* 558 (2018) 132–135.
- [8] W.C. Smith, A.K. Knecht, M. Wu, R.M. Harland, Secreted noggin protein mimics the Spemann organizer in dorsalizing *Xenopus* mesoderm, *Nature* 361 (1993) 547–549.
- [9] Y. Sasai, B. Lu, H. Steinbeisser, D. Geissert, L.K. Gont, E.M. De Robertis, *Xenopus* chordin: a novel dorsalizing factor activated by organizer-specific homeobox genes, *Cell* 79 (1994) 779–790.
- [10] E. Gazzero, V. Gangji, E. Canalis, Bone morphogenetic proteins induce the expression of noggin, which limits their activity in cultured rat osteoblasts, *J. Clin. Invest.* 102 (1998) 2106–2114.
- [11] T. Phan-Everson, F. Etoc, S. Li, S. Khodursky, A. Yoney, A.H. Brivanlou, E.D. Siggia, Differential Compartmentalization of BMP4/NOGGIN Requires NOGGIN Trans-epithelial Transport, *Developmental Cell*, 2021.
- [12] S. Tashiro, M.N.T. Le, Y. Kusama, E. Nakatani, M. Suga, M.K. Furue, T. Satoh, S. Sugiura, T. Kanamori, K. Ohnuma, High cell density suppresses BMP4-induced differentiation of human pluripotent stem cells to produce macroscopic spatial patterning in a unidirectional perfusion culture chamber, *J. Biosci. Bioeng.* 126 (2018) 379–388.
- [13] E. Nakatani, W. Yamazaki, S. Sugiura, T. Kanamori, K. Ohnuma, Modeling of differentiation pattern formation in human induced pluripotent stem cells mediated by BMP4 and its inhibitor noggin secreted from cells, *Biochem. Eng. J.* 176 (2021) 108159.
- [14] M. Bernfield, M. Götte, P.W. Park, O. Reizes, M.L. Fitzgerald, J. Lincecum, M. Zako, Functions of cell surface heparan sulfate proteoglycans, *Annu. Rev. Biochem.* 68 (1999) 729–777.
- [15] S. Paine-Saunders, B.L. Viviano, A.N. Economides, S. Saunders, Heparan sulfate proteoglycans retain Noggin at the cell surface: a potential mechanism for shaping bone morphogenetic protein gradients, *J. Biol. Chem.* 277 (2002) 2089–2096.
- [16] A. Woods, J.R. Couchman, Syndecans: synergistic activators of cell adhesion, *Trends Cell Biol.* 8 (1998) 189–192.
- [17] K. Takahashi, K. Tanabe, M. Ohnuki, M. Narita, T. Ichisaka, K. Tomoda, S. Yamanaka, Induction of pluripotent stem cells from adult human fibroblasts by defined factors, *Cell* 131 (2007) 861–872.
- [18] L.B. Zimmerman, J.M. De Jesús-Escobar, R.M. Harland, The Spemann organizer signal noggin binds and inactivates bone morphogenetic protein 4, *Cell* 86 (1996) 599–606.
- [19] A. Chakrabarti, G. Matthews, A. Colman, L. Dale, Secretory and inductive properties of *Drosophila* wingless protein in *Xenopus* oocytes and embryos, *Development* 115 (1992) 355–369.
- [20] D. Javelaud, A. Mauviel, Mammalian transforming growth factor- β s: smad signaling and physio-pathological roles, *Int. J. Biochem. Cell Biol.* 36 (2004) 1161–1165.
- [21] Y. Bi, C.H. Stuelten, T. Kiltz, S. Wadhwa, R.V. Iozzo, P.G. Robey, X.-D. Chen, M. F. Young, Extracellular matrix proteoglycans control the fate of bone marrow stromal cells, *J. Biol. Chem.* 280 (2005) 30481–30489.
- [22] S. Takada, S. Fujimori, T. Shinozuka, R. Takada, Y. Mii, Differences in the secretion and transport of Wnt proteins, *J. Biochem.* 161 (2017) 1–7.
- [23] A.M. Nesterenko, E.E. Orlov, G.V. Ermakova, I.A. Ivanov, P.I. Semenyuk, V. N. Orlov, N.Y. Martynova, A.G. Zaraisky, Affinity of the heparin binding motif of Noggin1 to heparan sulfate and its visualization in the embryonic tissues, *Biochem. Biophys. Res. Commun.* 468 (2015) 331–336.
- [24] M.C. Fisher, Y. Li, M.R. Seghatolslami, C.N. Dealy, R.A. Kosher, Heparan sulfate proteoglycans including syndecan-3 modulate BMP activity during limb cartilage differentiation, *Matrix Biol.* 25 (2006) 27–39.
- [25] S. Paine-Saunders, B.L. Viviano, J. Zupcich, W.C. Skarnes, S. Saunders, glypican-3 controls cellular responses to Bmp4 in limb patterning and skeletal development, *Dev. Biol.* 225 (2000) 179–187.